IOSR Journal of Engineering (IOSRJEN) **www.iosrjen.org**
ISSN (e): 2250-3021, ISSN (p): 2278-8719
Vol. 09, Issue 1 (January. 2019), ||V (I) || PP 47-53

Synthesis, Morphology and Thermal Properties of Tin Nanoparticles on a Carbon Matrix

A.V. Zaikovskii, M.A. Morozova, I.E. Naidenov, and S.A. Novopashin
Kutateladze Institute of Thermophysics, Novosibirsk, Russian Federation
Corresponding Author: A.V. Zaikovskii

Abstract: Tin nanoparticles on a carbon matrix were synthesized by the plasma-arc method. The synthesized material was characterized by the methods of transmission microscopy (TEM), X-ray phase analysis (XRD), and thermogravimetry (TGA). According to analysis of TEM images, tin nanoparticles are surrounded by a shell of material, less dense than tin, but denser than a carbon matrix. The size distribution functions of nanoparticles and their shells were measured. The average diameter of nanoparticles was 12 nm, and the thickness of shells was 3 nm. The melting point of nanoparticles and heat of phase transition were measured in accordance with the TGA data. It is shown that the synthesized material retains its properties at moderate overheating.

Date of Submission: 24-12-2018 Date of acceptance: 09-01-2019

I. INTRODUCTION

The use of phase transition heat for the storage of thermal energy and intensification of heat transfer processes is one of the most efficient methods. In recent years, the field of increasing coolant efficiency has been intensively developed due to addition of particles that have a phase transition temperature within the range of temperature change to the base medium [1, 2]. To preserve the particle shape, prevent particle crushing during melting, and eliminate possible chemical reactions with the carrier medium and walls of the channels, the technology of particle encapsulation in an inert shell is used. To increase the rate of heat transfer, the micron-sized particles are used.

Most publications in the field of synthesis and practical use consider the substances with a melting point in the range of 10–70°C. Such materials are already used in heat transfer processes both when adding such particles to the base heat-carrying medium [2], and directly as a charge, for example, in construction [1] or textile industry [3, 4].

Microencapsulation is a process in which microscopic particles or droplets are surrounded by a coating or embedded in some matrix, forming the capsules with certain properties. Depending on the physical-chemical properties of the core, composition of the shell and used encapsulation technologies, there can be various types of particles, among which the simple spheres are the most common type for production and applications.

The choice of core material depends on application and it should take into account the heat of melting, density, thermal conductivity, heat capacity, toxicity, corrosion and fire resistance. Since different materials exhibit different toxicological and reagent properties, it is extremely important to determine these properties in order to select a suitable shell material. The most commonly used materials are paraffins [5, 6], fatty acids [7], and hydrated salts [8].

The processes of microencapsulation are usually divided into two groups: chemical and physical processes. Physical methods are the spray drying and fluidized bed processes that initially do not allow formation of particles with a diameter less than 100 μm. Chemical processes include interfacial polymerization, in situ polymerization, coacervation, phase separation, suspension polymerization, and others. The chemical methods are mainly used [1, 9-13].

The transition to the fast heat transfer processes requires a transition from micron-sized particles to nanoparticles. To turn to other temperature ranges, it is necessary to develop the technologies based on other materials.

The current work is aimed at the synthesis of tin nanoparticles on a carbon matrix as a possible material with phase transition corresponding to higher temperatures than that of the used materials. Note that the tin-carbon composite is also interesting as an anode material in lithium-ion batteries [14].

II. EXPERIMENTAL SETUP AND MEASUREMENT METHODS

The synthesis of tin particles on a carbon matrix was implemented by the plasma-arc method [15]. The plasma-arc reactor is a vacuum chamber equipped with a forepump, which allows reaching vacuum of 10^{-2} Torr. The synthesis is carried out in an inert gas; for this purpose, the chamber is filled with helium to the required

pressure. In the reactor, there are two electrodes with an arc discharge, glowing between them. One of the electrodes is mobile graphite rod with a diameter of 20 mm; the second stationary electrode (anode) is a rod with a diameter of 8 mm and length of 70 mm. This design allows adjustment of a distance between the electrodes to maintain the arc discharge. A high-current metal-ceramic hermetic inlet is used to supply current to the reactor. A cylindrical copper circuit of water cooling is located around the electrodes. On the inner side of the circuit there is a removable stainless steel screen for collecting synthesis products. An adjustable DC source is used as the power source. The determining parameters of synthesis are the geometry and composition of electrodes, buffer gas and its pressure, and electrical characteristics of the discharge.

The synthesis was implemented with the following parameters: discharge current of 145 A; distance between the electrodes was regulated to maintain the arc voltage of about 20 V; helium pressure was 50 torr. The anode was a graphite rod with an axial bore filled with a mixture of ground tin and graphite in a 1: 1 weight ratio. Spraying the anode leads to formation of atomic components of carbon and tin in the arc. Diffusion and convection of atomic components in the buffer gas leads to cooling and heterogeneous condensation. Further, the condensation products are deposited on a cooled screen. The synthesized material consists of tin nanoparticles in a carbon matrix.

To analyze the morphology of synthesized material, a JEM-2010 transmission electron microscope with a grating resolution of 0.14 nm was used; accelerating voltage was 200 kV. The X-ray phase analysis was performed with a Bruker D8 Advanced diffractometer, with increments of $2\Theta = 0.05$ o and accumulation time of 1 and 3 s at each point, using a Lynexeye linear detector (1D); monochromatic radiation of the CuK_{α} copper line was used. Thermogravimetric measurements and differential scanning calorimetry were performed using a NETZSCH STA 409 device with a heating rate of 10°C/min, calibrated on high-purity metals: In, Sn, Bi, and Zn.

III. RESULTS AND ANALYSIS

A part of material obtained was subjected to annealing at the temperature of 800°C for two hours with free access of air. As a result, the carbon matrix, forming CO_2, evaporates from the sample. Tin and its oxide contained in the sample are oxidized to the oxide with the maximal oxidation degree: SnO_2. A change in mass due to annealing allows us to calculate the mass composition of the initial material. The calculated mass fraction of tin in the initial sample was 33.9%.

Figures 1-3 represent images of samples obtained on a transmission electron microscope with different spatial resolution. It can be seen there that some particles are surrounded by a shell of a lower density, followed by an amorphous carbohydrate matrix. We should note that in some images a crystal structure can be seen (Fig. 2, 3). After annealing in an oxygen-containing atmosphere, the carbon shell is removed and tin is oxidized. An example of a photograph of the annealed material is shown in Fig. 4. Note that the crystal structure of particles is also clearly visible.

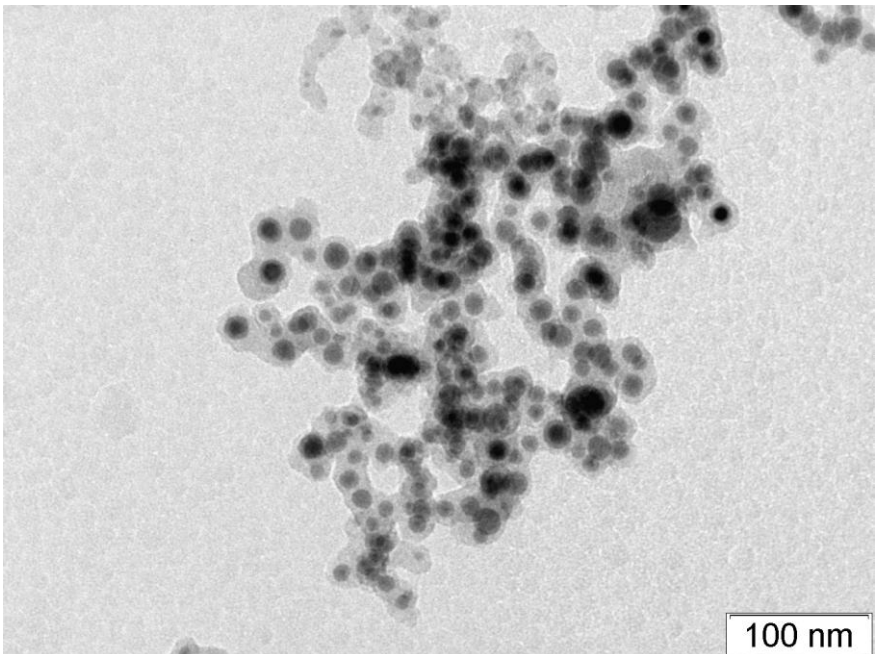

Fig. 1. Morphology of synthesized material.

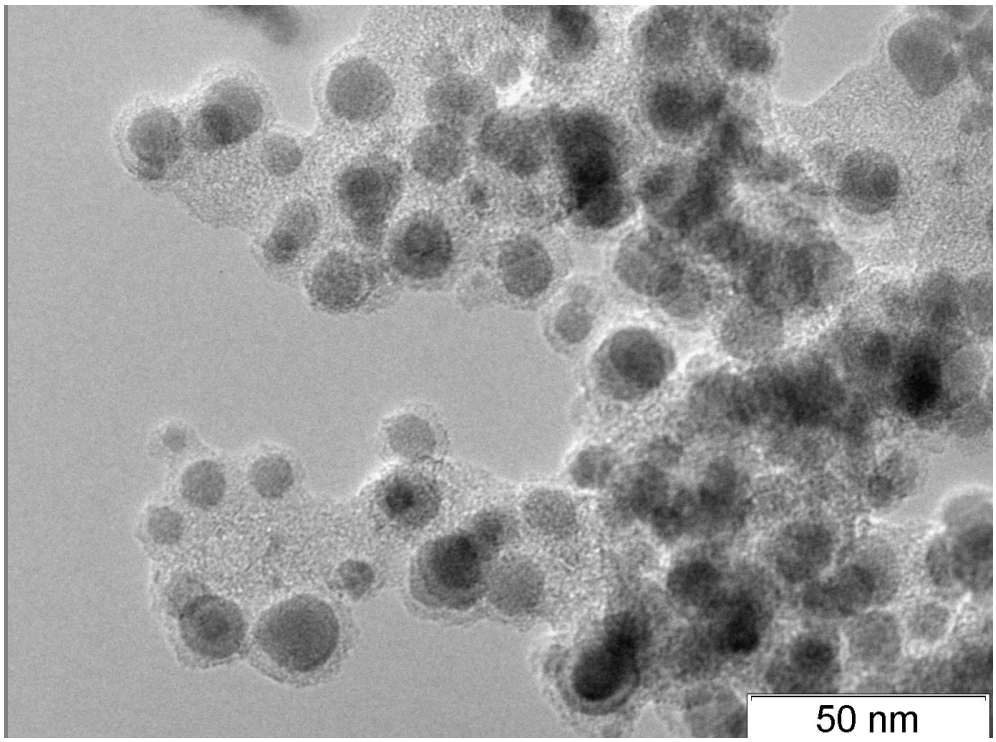

Fig. 2 Morphology of synthesized material with large magnification.

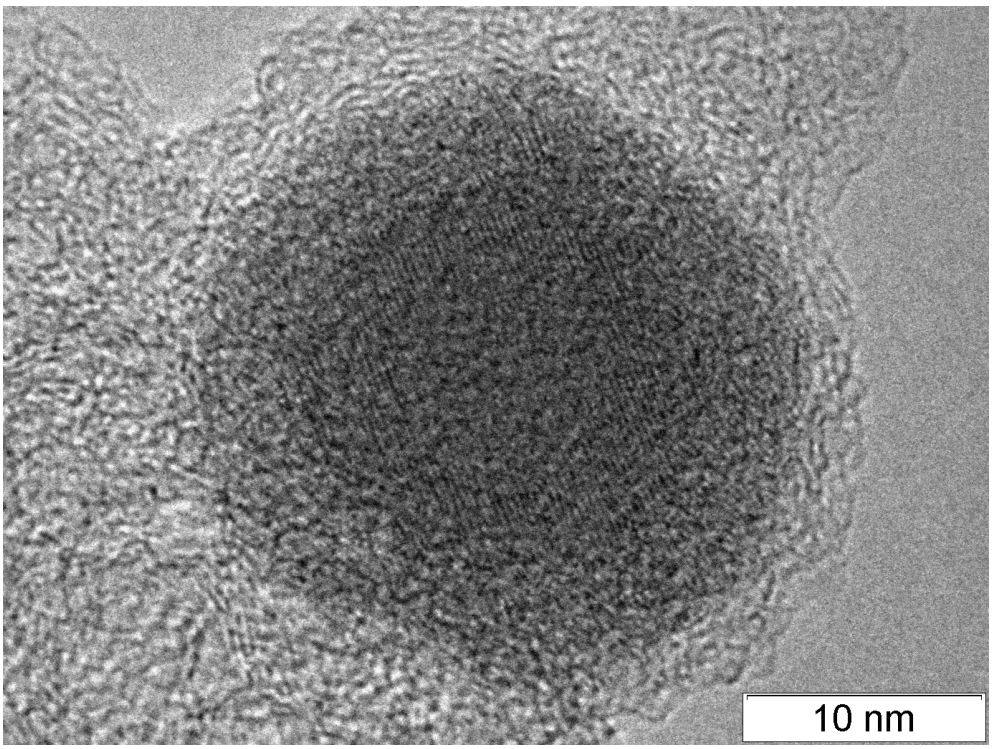

Fig. 3 Morphology of a separate particle with a shell.

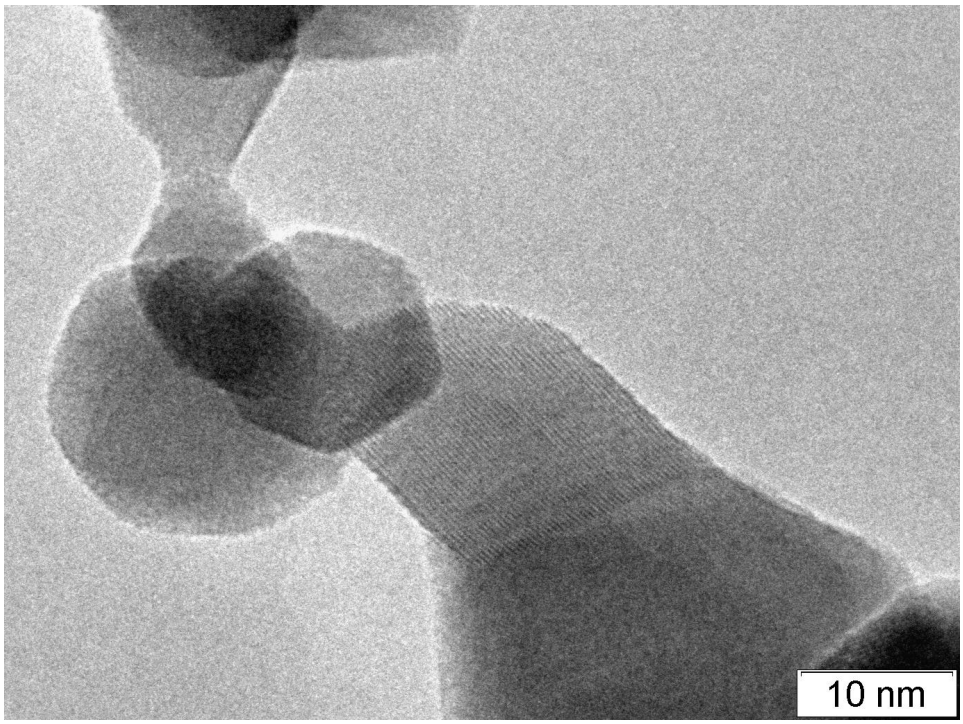

Fig. 4. Material after annealing.

The obtained images allow measurement of the size distribution function of synthesized particles and analysis of the crystal structure of synthesized particles. The size distribution function of nanoparticles is shown in Fig. 5.

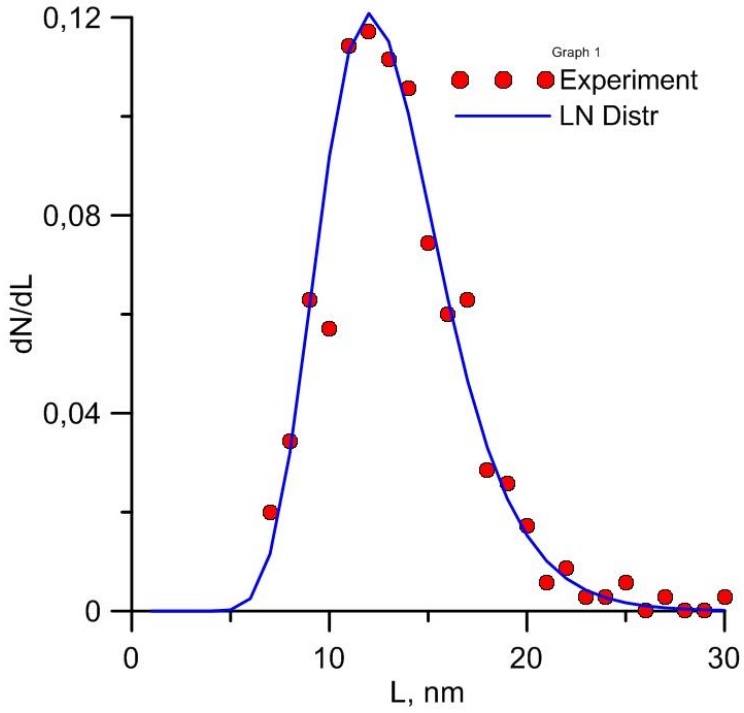

Fig. 5. Size distribution of particles.

For a comparatively smaller sampling of particles with a well-distinguishable shell together with the external dimensions it is possible to measure the core diameter and, accordingly, the wall thickness. According to the measurements, the average wall thickness is about 3 nm.

The XRD spectrum (Fig. 6) shows the distinct peaks corresponding to graphite and β-modification of tin. The absence of peaks, corresponding to tin oxide, in the spectrum suggests that if tin oxide is available in the synthesized material, it is in the amorphous state.

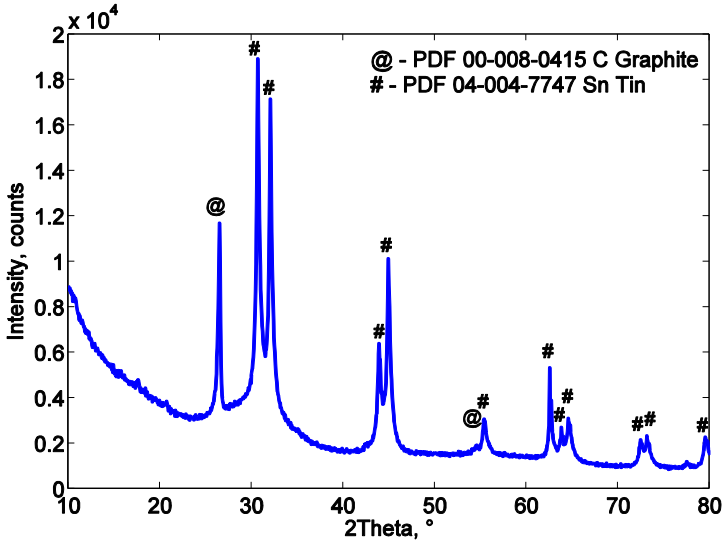

Fig. 6. The XRD spectrum.

Measuring the peak half-width allows us to calculate the average length of coherent scattering. For the first five peaks, an average value of 19 nm was obtained. The difference with the average value obtained directly from the TEM images is probably caused by the fact that the larger particles make a greater contribution to the peak intensity in the XRD measurements.

The heating curve obtained by thermogravimetric analysis is shown in Fig. 7. Heat absorption near the melting point of tin (231.9°C) indicates that the phase transition temperature retains its value for nanoparticles. The calculation of melting enthalpy by the peak integral gave the value of 4.7 J/g. Taking into account that the amount of tin per 1 g of material is 33.9%, and enthalpy of tin mass melting is 59.55 J/g, we obtain that experimentally detected heat of melting is about 23% of the theoretical value. A significant change in the heat of melting may be caused by two reasons. Firstly, tin is partially oxidized and oxide does not contribute to the observed thermal effect. Secondly, enthalpy of phase transition for particles of the nanometer size may differ from the corresponding value for the mass. For a quantitative analysis of contributions of both mechanisms to the observed phenomenon of a decrease in the heat of phase transition, the additional experiments are required.

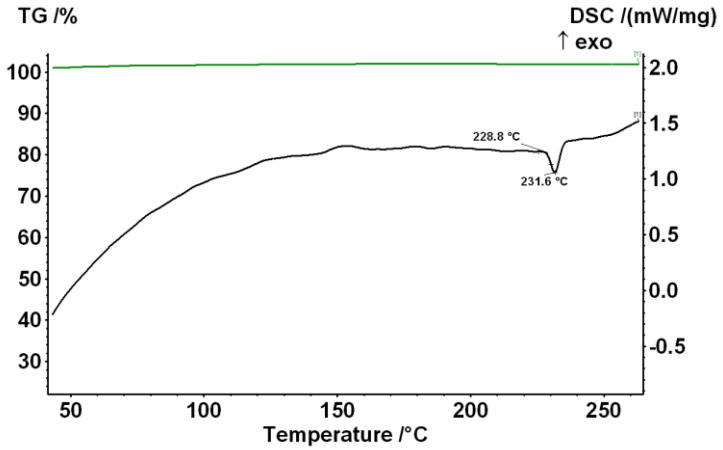

Fig. 7. The XRD curve of heat absorption.

When samples were heated to the temperature exceeding the melting point by several degrees, the material morphology did not change during cooling (Fig. 8a). However, after heating in an inert atmosphere to the temperature of 265°C, a marked change in the morphology of individual particles occurred. Heating leads to violation of the shell integrity, and metal can leave a cell in the carbon matrix, leaving a cavity behind (Fig. 8b). When heated to the temperature of 1250°C, this phenomenon is observed for most particles. Many hollow carbon shells can be seen in Fig. 9a. The surface tension promotes association of "come out" droplets, which leads to formation of large spherical particles with the sizes of 100–500 nm (Fig. 9b).

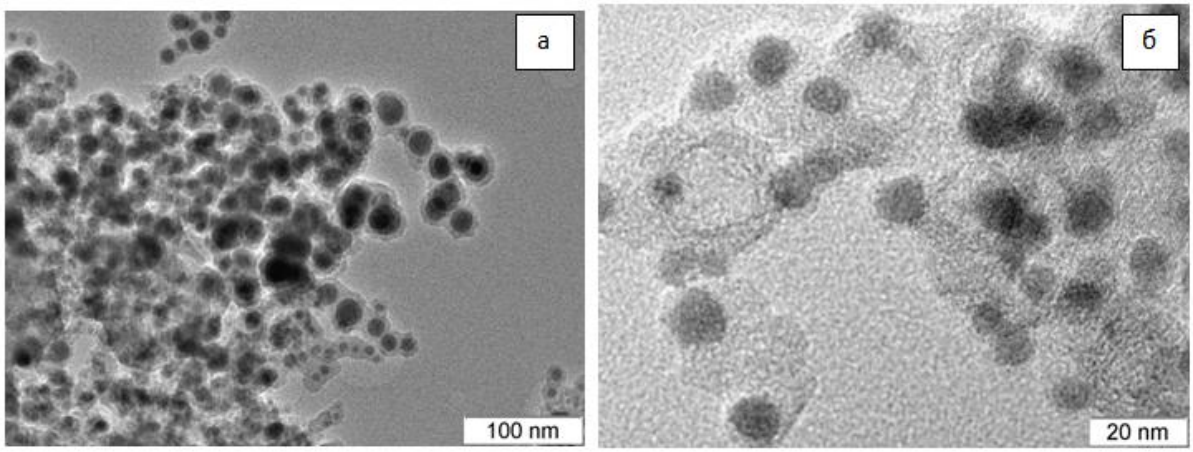

Fig. 8. Morphology of material at heating to 235°C (a) and 265°C (в).

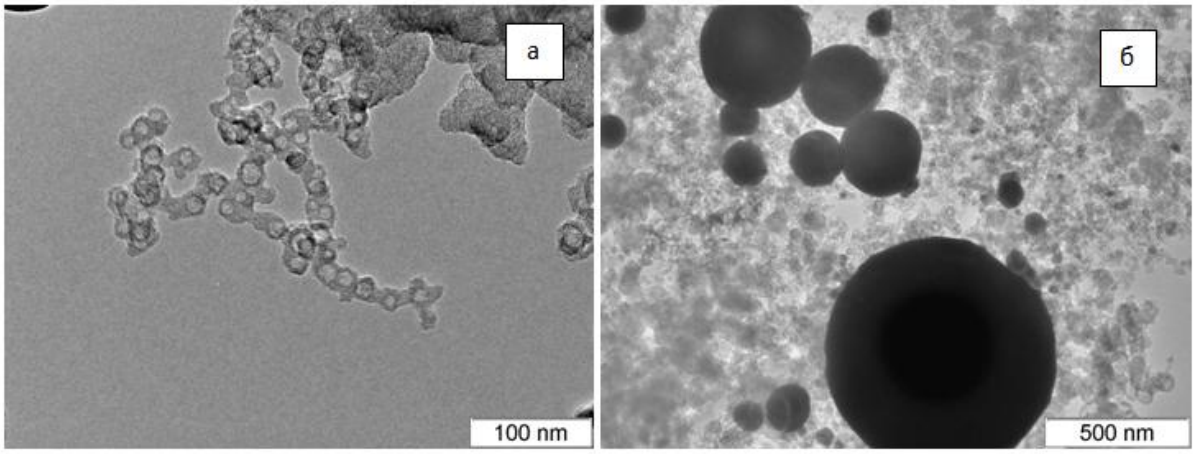

Fig. 9. Material after heating to 1250°C.

IV. CONCLUSIONS

Plasma-arc synthesis of tin nanoparticles on a carbon matrix has been implemented. The morphology of synthesized material and its thermal properties were investigated. The average diameter of nanoparticles was 12 nm. It is shown that the melting point does not change at transition to nanoscales. The measured heat of phase transition was not higher than 25% of phase transition heat for the mass. It is shown that the synthesized material retains its morphology and thermal properties at moderate overheating.

REFERENCES

[1]. Jahns E. Microencapsulated phase change material. In: International Energy Agency Energy Conversation through Energy Storage Programm(ECES), Annex 10: Fourth Workshop 1999.
[2]. Zhang P, Ma ZW, Wang RZ. An overview of phase change material slurries:
[3]. MPCS and CHS. Renewable and Sustainable Energy Reviews.2010;14:598-614.
[4]. Shin Y, Yoo D-I, Son K. Development of thermoregulating textile materials with microencapsulated phase change materials (PCM). II. Preparation and application of PCM microcapsules. Journal of Applied Polymer Science. 2005;96:2005-10.
[5]. Shin Y, Yoo D-I, Son K. Development of thermoregulating textile materials with microencapsulated phase change materials (PCM). IV. Performance properties and hand of fabrics treated with PCM microcapsules. Journal of Applied Polymer Science. 2005;97:910-5.
[6]. Zhang XX, Tao XM, Yick KL, Fan YF. Expansion space and thermal stability of microencapsulated n-octadecane. Journal of Applied Polymer Science. 2005;97:390-6.
[7]. Fan YF, Zhang XX, Wu SZ, Wang XC. Thermal stability and permeability of microencapsulated n-octadecane and cyclohexane. Thermochimica Acta. 2005;429:25-9.
[8]. Yuan YC, Rong MZ, Zhang MQ. Preparation and characterization of microencapsulated polythiol. Polymer. 2008;49:2531-41.

[9]. Yadav SK, Suresh AK, Khilar KC. Microencapsulation in polyurea shell by interfacial polycondensation. AIChE Journal. 1990;36:431-8.
[10]. Zhang X-X, Tao X-M, Yick K-L, Wang X-C. Structure and thermal stability of microencapsulated phase-change materials. Colloid & Polymer Science. 2004;282:330-6.
[11]. Song Q, Li Y, Xing J, Hu JY, Marcus Y. Thermal stability of composite phase change material microcapsules incorporated with silver nano-particles. Polymer. 2007;48:3317-23.
[12]. 11.Wang J-P, Zhao X-P, Guo H-L, Zheng Q. Preparation of Microcapsules Containing Two-Phase Core Materials. Langmuir. 2004;20:10845-50.
[13]. Rao Y, Lin G, Luo Y, Chen S, Wang L. Preparation and thermal properties of microencapsulated phase change material for enhancing fluid flow heat transfer. Heat Transfer-Asian Research. 2007;36:28-37.
[14]. Park S-J, Shin Y-S, Lee J-R. Preparation and Characterization of Microcapsules Containing Lemon Oil. Journal of Colloid and Interface Science. 2001;241:502-8.
[15]. Wu Xiaohui, Liu Zhiliang, Zheng Jie, Li Xingguo and Shi Zujin Arc-discharge synthesis of dual-carbonaceouslayer-coated tin nanoparticles with tunable structures and high reversible lithium storage capacity. J. Mater. Chem. A, 2017, 5, 13769–13775.
[16]. R.V. Gulyaev, E.M. Slavinskaya, S.A. Novopashin, D.V. Smovzh, A.V. Zaikovskii, D.Yu. Osadchii, O.A. Bulavchenko, S.V. Korenev, A.I. Boronin. Highly active PdCeOx composite catalysts for low-temperature CO oxidation, prepared by plasma-arc synthesis // Applied Catalysis B: Environmental, 2014, Vol. 147, pp 132– 143.

A.V. Zaikovskii. “ Synthesis, Morphology and Thermal Properties of Tin Nanoparticles on a Carbon Matrix. ” IOSR Journal of Engineering (IOSRJEN), vol. 09, no. 01, 2019, pp. 47-53.